



Modeling shield immunity to reduce COVID-19 epidemic spread

Joshua S. Weitz^{1,2,3}✉, Stephen J. Beckett¹, Ashley R. Coenen², David Demory¹, Marian Dominguez-Mirazo^{1,4}, Jonathan Dushoff^{1,5,6}, Chung-Yin Leung^{1,2}, Guanlin Li^{2,4}, Andreea Măgălie^{1,4}, Sang Woo Park⁷, Rogelio Rodriguez-Gonzalez^{1,4}, Shashwat Shivam⁸ and Conan Y. Zhao^{1,4}

The COVID-19 pandemic has precipitated a global crisis, with more than 1,430,000 confirmed cases and more than 85,000 confirmed deaths globally as of 9 April 2020^{1–4}. Mitigation and suppression of new infections have emerged as the two predominant public health control strategies⁵. Both strategies focus on reducing new infections by limiting human-to-human interactions, which could be both socially and economically unsustainable in the long term. We have developed and analyzed an epidemiological intervention model that leverages serological tests^{6,7} to identify and deploy recovered individuals⁸ as focal points for sustaining safer interactions via interaction substitution, developing what we term ‘shield immunity’ at the population scale. The objective of a shield immunity strategy is to help to sustain the interactions necessary for the functioning of essential goods and services⁹ while reducing the probability of transmission. Our shield immunity approach could substantively reduce the length and reduce the overall burden of the current outbreak, and can work synergistically with social distancing. The present model highlights the value of serological testing as part of intervention strategies, in addition to its well-recognized roles in estimating prevalence^{10,11} and in the potential development of plasma-based therapies^{12–15}.

In the absence of reliable pharmaceutical interventions against SARS-CoV-2, multiple public health strategies are being deployed to slow the coronavirus pandemic^{1,5,16}. These strategies can be broadly grouped into two approaches: mitigation and suppression. Mitigation includes a combination of social distancing (including school and university closures), case testing and symptomatic case isolation to reduce epidemic spread and burden on hospitals. Mitigation is intended to lessen an outbreak. However, the number of cases might still overwhelm health services⁵. Some jurisdictions have either preemptively or reactively adopted a combination of travel restrictions (shown to be effective in curtailing dispersion if implemented early enough^{17,18}) and suppression, which involves imposing complete shutdowns of the bulk of non-essential services for extended periods. Suppression strategies have led to marked decreases in new case rates in the short term by combining case isolation, quarantine, use of separate facilities for treating COVID-19 patients and large-scale

viral testing to reduce transmission¹⁹. Suppression also comes with considerable community and economic costs, for example, threatening social order and affecting employment and other factors, especially among disadvantaged groups²⁰.

Here, we propose an approach to limit transmission, which is both complementary to and intended to lessen the multifaceted costs of mitigation and suppression. The core idea is to leverage a mechanism of ‘interaction substitution’ by identifying recovered individuals who have protective antibodies to SARS-CoV-2 and deploying them back into the community. The intention of this strategy is to develop population-level ‘shield immunity’ by amplifying the proportion of interactions with recovered individuals relative to those of individuals of unknown status (Fig. 1). Here, we assume that recovered individuals (virus-negative and antibody-positive) can safely interact with both susceptible and infectious individuals, in effect substituting interactions with susceptible and infectious individuals for interactions with recovered individuals. This intervention strategy is initially local in scope and scales with outbreak size, given that the potential effects of shield immunity increase following a local outbreak. A summary of the main findings, limitations and implications of the model is shown in Table 1.

To illustrate the core concept of shield immunity, we consider an epidemic model in which individuals preferentially substitute their interactions with identified or strategically located recovered individuals. Hence, rather than mixing at random, we consider a relative preference of $1 + \alpha$ that a given individual will interact with a recovered individual in what would otherwise be a potentially infectious interaction. This type of interaction substitution is equivalent to assuming an effective contact rate ratio of $1 + \alpha$ for recovered individuals relative to the rest of the population. The dynamics of the fraction of susceptible (S), infectious (I) and recovered (R) individuals are

$$\begin{aligned}\dot{S} &= -\beta \frac{SI}{1+\alpha R} \\ \dot{I} &= \beta \frac{SI}{1+\alpha R} - \gamma I \\ \dot{R} &= \gamma I\end{aligned}$$

such that when $\alpha=0$ we recover the conventional SIR model given transmission rate β and recovery rate γ . Note that the denominator

¹School of Biological Sciences, Georgia Institute of Technology, Atlanta, GA, USA. ²School of Physics, Georgia Institute of Technology, Atlanta, GA, USA.

³Center for Microbial Dynamics and Infection, Georgia Institute of Technology, Atlanta, GA, USA. ⁴Interdisciplinary Graduate Program in Quantitative Biosciences, Georgia Institute of Technology, Atlanta, GA, USA. ⁵Department of Biology, McMaster University, Hamilton, Ontario, Canada. ⁶DeGroote Institute for Infectious Disease Research, McMaster University, Hamilton, Ontario, Canada. ⁷Department of Ecology and Evolutionary Biology, Princeton University, Princeton, NJ, USA. ⁸School of Electrical and Computer Engineering, Georgia Institute of Technology, Atlanta, GA, USA.

✉e-mail: jsweitz@gatech.edu

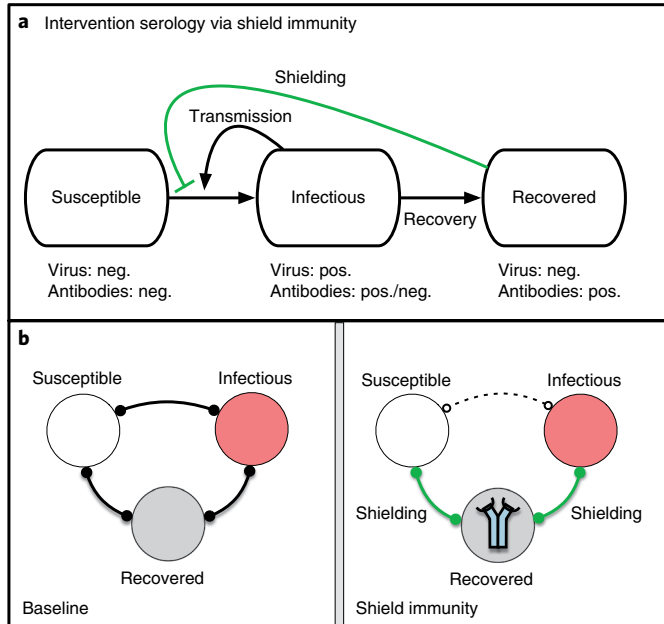


Fig. 1 | Simplified schematic of intervention serology via shield immunity.

a, Population dynamics of susceptible, infectious and recovered, in which recovered individuals reduce contact between susceptible and infectious individuals. Arrows denote flows between population-level compartments. **b**, Individual views of the baseline scenario (left) and shielding scenario (right), in which the identification, designation and deployment of recovered individuals is critical to enabling susceptible-recovered and infectious-recovered interactions to replace susceptible-infectious interactions. Bonds denote interactions between individuals. In the 'Shield immunity' panel, the icon in the recovered individuals denotes the identification of individuals with protective antibodies, and hence the enhanced contribution of such individuals to shield immunity in contrast to the 'Baseline' panel.

$1 + \alpha R$ can be thought of as $S + I + R + \alpha R$. Given that $S + I + R = 1$, this is equivalent to the term $1 + \alpha R$. Figure 1 illustrates shield immunity impacts on a SIR epidemic with $\mathcal{R}_0 = 2.5$ (\mathcal{R}_0 is the basic reproduction number). In this SIR model, shield immunity reduces the epidemic peak and shortens the duration of epidemic spread. Shielding in this context acts as a negative feedback loop, given that the effective reproduction number is given by $\mathcal{R}_{\text{eff}}(t)/\mathcal{R}_0 = S(t)/(1 + \alpha R(t))$. As a result, interaction substitution increases as recovered individuals increase in number and are identified. For example, in the case of $\alpha=20$, the epidemic concludes with less than 20% infected in contrast to the final size of ~90% in the baseline scenario without shielding (Fig. 2).

We also examined 'flexible' and 'fixed' shielding as potential alternative interaction substitution mechanisms (see Methods). A flexible shielding mechanism accounts for enhanced time-varying interaction rates of recovered individuals by a factor of $(1 + \alpha)$ relative to the interaction rate of other individuals, while keeping the total contact rate equal to that of the baseline (explicitly accounting for a strict substitution of interaction). A fixed shielding mechanism considers enhanced time-fixed interaction rates of recovered individuals by a factor of $(1 + \alpha)$ relative to the baseline rate, while keeping the total contact rate equal to that of the baseline (again explicitly accounting for strict substitution of interactions). Extended Data Fig. 1 shows that shielding is robust to these alternative scenarios, and potentially even more effective. For example, in a scenario of fixed shielding with $\alpha=3$, recovered individuals sustain four times as many contacts relative to their pre-intervention baseline,

Table 1 | Policy summary

Background	Mitigation and suppression have emerged as the primary means to control the pandemic spread of COVID-19, raising questions of sustainability and exit strategies. Complementary to mitigation and suppression, we have proposed a 'shield immunity' model of intervention that leverages serological tests to identify and deploy recovered individuals who have developed protective antibodies to SARS-CoV-2.
Main findings and limitations	Serological testing is essential to identifying individuals who have been infected, recovered and are immune (in the near term) to SARS-CoV-2. Several scenarios have been explored that show substantive decreases in cases, hospitalizations, and deaths compared to baseline given enhanced interactions with recovered individuals that reduce the risk of transmission. As with all modeling studies, our predictions come with reasonable assumptions; nonetheless, controlling the course of the epidemic could benefit from identifying seropositive individuals and integrating their behavior into multifaceted intervention approaches.
Policy implications	Our findings reinforce the need for large-scale, serological testing initiatives to identify individuals who have recovered from COVID-19. Although questions remain about the duration and effectiveness of immunity, strategic identification and deployment of recovered individuals represents an opportunity to reduce transmission for the collective good. Initiating large-scale serological testing initiatives is key to proactive approaches to end the COVID-19 pandemic and enable economic re-engagement.

ensuring the final outbreak concludes with less than 25% of the population having been infected compared to the expectation of ~90% in the absence of shielding. We use our core shielding model as the basis for application to COVID-19, as it represents the conservative benefits of shielding; however, detailed mixing and substitution models could also lead to further variations of this model, such as in spatially explicit domains or on networks^{21–24}.

Here, we apply our model of shield immunity to the epidemiological dynamics of the COVID-19 pandemic. For simplicity, we ignore births and other causes of death. We consider a population of susceptible (S), exposed (E), infectious asymptotically (I_a), infectious symptomatically (I_s) and recovered R who are free to move without restrictions in a 'business as usual' scenario. A subset of symptomatic cases will require hospital care, which we further divide into subacute (I_{hsu}) and critical and/or acute (requiring intensive care unit (ICU) intervention, I_{hcri}) cases. We assume that a substantial fraction of critical cases will die. Age-stratified risk of hospitalization and acute cases are adapted from the values from ref. ⁵, which models potential outcomes in the United Kingdom and the United States. The full model incorporating shield immunity (see Methods and Extended Data Fig. 2) differs from conventional SIR models with social distancing or case isolation interventions. The rate of transmission is reduced by a factor of $1/(N_{\text{tot}} + \alpha R_{\text{shields}})$ where N_{tot} denotes the fraction of the population in the circulating baseline, and R_{shields} denotes the total number of recovered individuals between the ages of 20 and 60 years (a subset of the total recovered population). In this model, we assume that all recovered individuals have immunity, but that only a subset are able to facilitate interaction substitutions. The model assumes that the individuals in the circulating pool are not interacting with hospitalized patients.

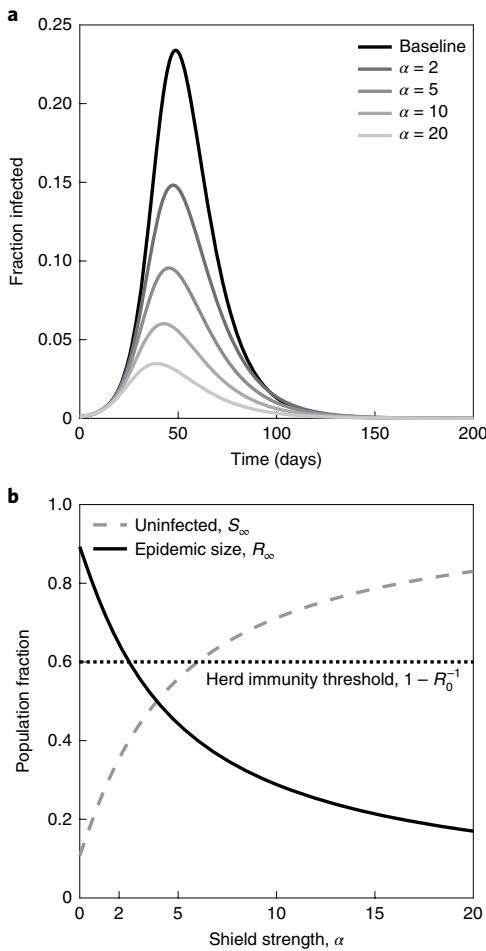


Fig. 2 | Shield immunity dynamics in a SIR model. **a**, Infectious case dynamics with different levels of shielding, α . **b**, Final state of the system as a function of α . In both panels, $\beta = 0.25$ (transmission rate 1/day) and $\gamma = 0.1$ (recovery rate 1/day). S , susceptible individuals; I , infectious individuals; R , recovered individuals.

Interactions with patients in the hospital setting need to be incorporated into specific implementation scenarios with healthcare workers²⁵. The baseline epidemiological parameters, age-stratified risk and population structure are provided in Supplementary Tables 1 and 2 and in the code (available on GitHub at https://github.com/WeitzGroup/covid_shield_immunity).

We use the baseline epidemiological parameters^{5,26–29} (Supplementary Tables 1 and 2) and seed an outbreak with a single exposed individual until the outbreak reaches 0.1% total prevalence (10,000 individuals infected out of a population of 10,000,000, at which point a shielding strategy is implemented). Outbreak scenarios differ in transmission rates, with $\mathcal{R}_0 = 1.57$ and 2.33 in the low-transmission and high-transmission scenarios, respectively. Early estimates of \mathcal{R}_0 from Wuhan are consistent with a 95% confidence interval (CI) of between 2.1 and 4.5 (ref. ³⁰), putting our high-transmission scenario on the conservative end of estimated ranges. However, the \mathcal{R}_0 of the high-transmission scenario we examine here is consistent with the range of 2.0–2.6 considered in ref. ⁵, and with the median of $\mathcal{R}_0 = 2.38$ (95% CI, 2.04–2.77) as estimated via stochastic model fits to outbreak data in China that account for undocumented transmission²⁸. Moreover, given that control measures reduce transmission¹⁹, our low-transmission scenario is consistent with estimates of $\mathcal{R}_0 = 1.36$ (95% CI, 1.14–1.63) in China from 24 January to 3 February after travel restrictions

and other measures were implemented. Figure 3 shows the results of comparing shielding interventions to the baseline outbreak. As in the simple SIR model, shielding on its own could potentially decrease epidemic burden across multiple metrics, decreasing both the total impact and shortening the peak event. In a population of size 10,000,000 for the high-transmission scenario, the final epidemic predictions are 71,000 deaths in the baseline case compared with 58,000 deaths given intermediate shielding ($\alpha = 2$) and 20,000 deaths given enhanced shielding ($\alpha = 20$). In a population of size 10,000,000 for the low-transmission scenario, the final epidemic predictions from our model are 50,000 deaths in the baseline case compared with 34,000 deaths given intermediate shielding and 8,300 deaths given enhanced shielding. The majority of deaths are of individuals aged 60 years and older, despite the lower fraction of individuals in those ranges (Fig. 3), which is consistent with estimates in related COVID-19 models^{5,27,28} and from the outbreaks in Italy and China³¹. Our simulation results consider effects of shielding alone, whereas ongoing restrictions, such as social distancing and shelter-in-place orders, will help to further reduce interaction rates. The effectiveness of shielding depends on the product of multiplying the number of potential shields identified and their effective substitutability, that is, $\alpha R_{\text{shields}}$, combining identification of and interaction rate by recovered individuals.

The population-scale effects of shielding relies on multiple factors, including demographic distributions, the fraction of asymptomatic transmission^{26,28} and the duration of immunity. We find that populations with a strongly right-shifted demographic distribution could potentially receive increased benefits from shielding. Even though there are fewer recovered individuals between the ages of 20 and 60 to draw from in right-shifted demographic distributions than left-shifted demographic distributions, the effect of shield immunity is greater. We find that the relative reduction in deaths via shield immunity compared to the baseline scenario is proportional to the fraction of population over 60 years (see Methods for details on US state-level analyses and also Extended Data Fig. 3). Similar results are expected to hold for countries, such as Italy, where more than 23% of the population is older than 65 years and nearly 30% is older than 60 years. Shield immunity is robust to variation in asymptomatic infection probabilities, which improves outcomes in models with varying baseline levels of asymptomatic transmission (Extended Data Figs. 4–6). In addition, our model assumes that immunity has fast onset (2–3 weeks) and is permanent in duration. Clinical work at Zhejiang University, China, suggests that seroconversion of total antibody, IgM and IgG antibodies developed with a median period of 15, 18 and 20 days post exposure, respectively, for symptomatic patients in a hospital³². The effects of shield immunity are robust in a scenario where the duration of immunity is four months or longer (Extended Data Figs. 7 and 8). Distinct control measures that extend the epidemic would probably influence the effectiveness of shield immunity given variation in immune responses at the individual level. The titer of protective antibodies in individuals infected with related betacoronaviruses (causing mild/moderate symptoms) reduced over a one-year period such that re-exposure can lead to re-infection³³, by contrast with evidence of multi-year immunity for individuals who have recovered from SARS³⁴. In addition, we emphasize that the accuracy of serological tests is essential. The benefits of shield immunity may be undermined if recovered individuals can be re-infected (even with little danger to themselves) or if these individuals are potentially misidentified, which could lead to interaction substitution with individuals who could infect others. This risk could be abrogated by combining serology with PCR testing methods.

In practice, shield immunity would not be implemented as a singular strategy; rather, multiple interventions will be used in parallel. We evaluated the synergistic potential of utilizing shield immunity in combination with social distancing. Social distancing

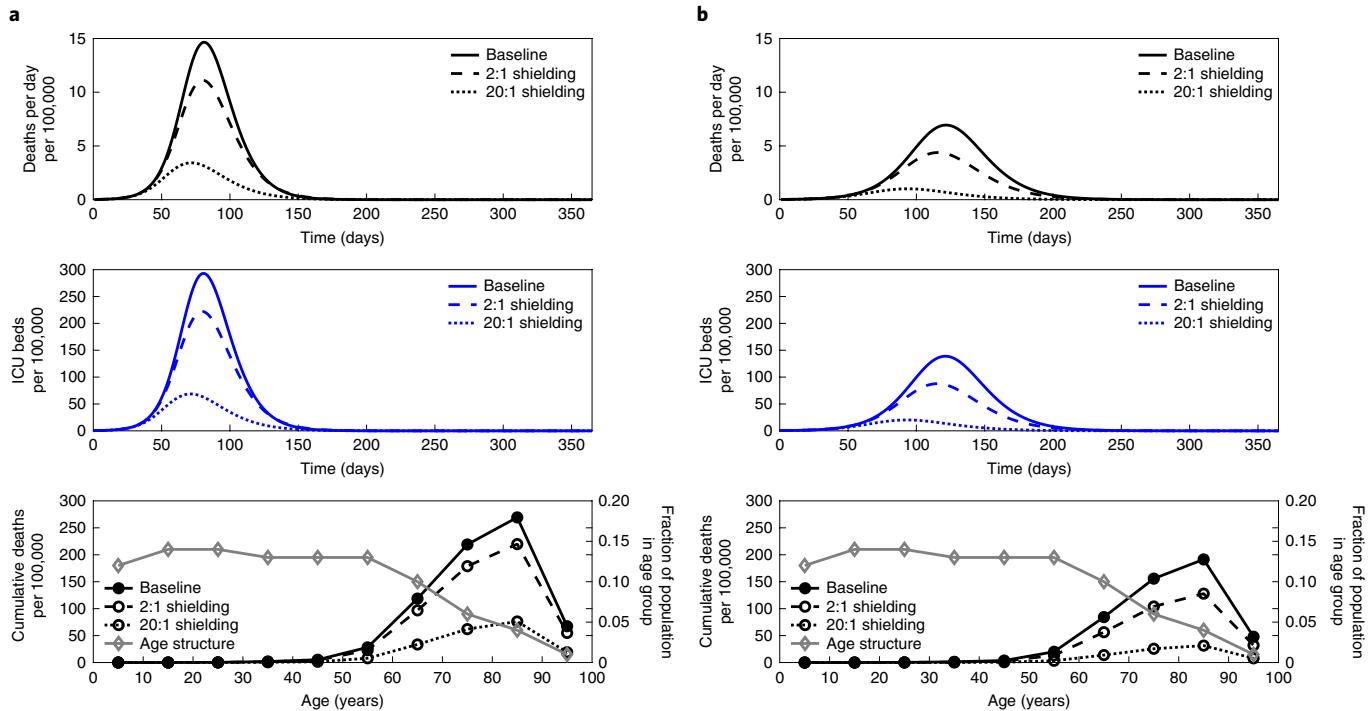


Fig. 3 | COVID-19 dynamics in a baseline scenario without interventions compared with two shield immunity scenarios, $\alpha = 2$ and $\alpha = 20$, including deaths, ICU beds needed and age distribution of fatalities. **a,b,** See Methods and Extended Data Fig. 1 for more details on the alternative scenarios with high transmission ($\mathcal{R}_0 = 2.33$) (a) and low transmission ($\mathcal{R}_0 = 1.57$) (b).

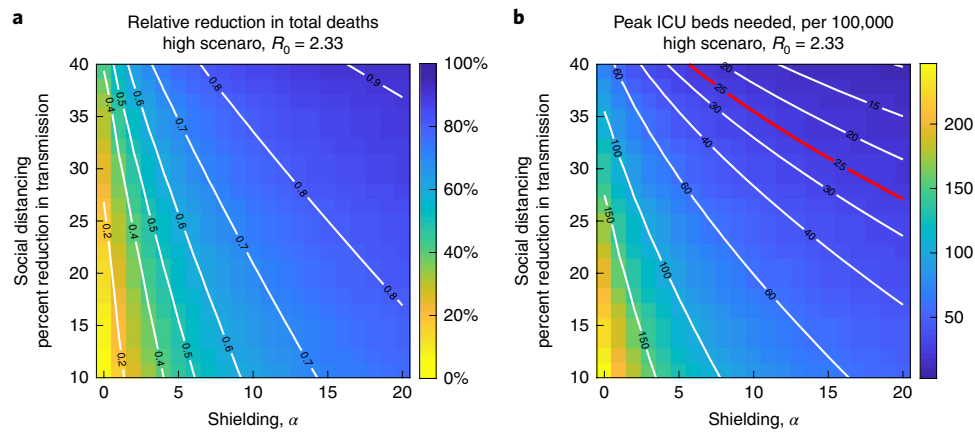


Fig. 4 | Impacts of combined interventions of shielding and social distancing in the high-transmission scenario. **a,** Fractional reduction in deaths compared to baseline for the high-transmission scenario ($\mathcal{R}_0 = 2.33$). **b,** Peak level of ICU beds needed per 100,000 individuals on a given day during the epidemic for the high-transmission scenario ($\mathcal{R}_0 = 2.33$). The red line denotes 25 ICU beds per 100,000 individuals as a demarcation point for surge capacity.

is modeled as a reduction in the transmission rates sustained over the post-intervention period. Shielding can augment social distancing, particularly when social distancing is largely ineffective (Fig. 4). For example, contour lines of reduction in total fatalities suggest that a combination of 10% reduction in transmission with $\alpha = 20$ is equivalent to a nearly 50% reduction in transmission in the absence of shield immunity. However, there is a compromise. Because social distancing reduces contacts and transmission, there are fewer recovered individuals when β is reduced by 50%. Nonetheless benefits of shielding accrue at all levels of social distancing. Social distancing and shield immunity could work in combination to improve outcomes in terms of expected hospitalization burden, suggesting a role for shield immunity in reducing transmission and reducing

the negative impacts of suppression-level social distancing policies. Finally, targeted shield immunity could also enhance population outcomes by focusing the effort of recovered individuals in subsets of the population. Heuristic solutions to an optimization formulation of targeted (age-specific) shield immunity in this model are shown in Extended Data Figs. 9 and 10. By preferentially targeting older individuals by shielding those at highest risk, it is possible to further reduce cumulative deaths by ~30%.

Population-wide serological testing is urgently needed. We have shown a rationale for serological testing as a means to facilitate interventions complementary to mitigation and suppression. Identifying and deploying recovered individuals represents an opportunity to slow transmission by developing population-level shield immunity.

Yet, logistical and social challenges must be addressed to implement shield immunity in practice. Accurate and rapid serological tests are needed at scale, including targeted surveys to identify essential workers and via population-level surveys. In evaluating the suitability of test features, high specificity is critical, so that people who are susceptible are not mistakenly identified as recovered (false positives). On 9 April 2020, the US Food and Drug Administration authorized emergency use of a SARS-CoV-2 antibody test with reported 96% specificity and 94% sensitivity (<https://www.fda.gov/media/136625/download>). There were no reported false positives out of 250 cases when combining IgG and IgM; however, this does come at the cost of decreased sensitivity. In practice, the positive predictive value will vary with prevalence, suggesting that deployment could be more effective among groups that appear to have elevated rates of current or past infection. The possibility of combining models of shield immunity with test accuracy and specificity warrants further exploration.

The potential scale of shield immunity depends on both the intrinsic epidemic dynamics, which drives the number of recovered individuals able to provide shield immunity, as well as the ability to accurately identify and deploy these individuals. As serological tests become widely available and, hopefully, improvements in specificity are made, new questions will be raised with respect to test prioritization and action-taking for those who test positive for protective antibodies. Public health authorities and governmental agencies need to consider how to best prioritize testing for those in critical roles, those with experience in disaster response, as well as individuals who have previously tested positive for SARS-CoV-2, who could return for both serology-based and viral-shedding assays. Positive confirmation of immunity and cessation of viral shedding could help identify and deploy a substantial proportion of the population as part of a shield immunity strategy, with the greatest concentration potentially co-located with areas in greatest need of intervention. Integrative strategies could consider the deployment of critical response workers with protective antibodies to help control new outbreaks, as was proposed for efforts to curb the spread of Ebola virus disease in West Africa in 2014³⁵.

We also recognize that there are considerable challenges to implementing interventions that aim to develop population-wide shield immunity. Nonetheless, the magnitude of the current public health and economic crisis demands large-scale action^{36,37}. The efficacy of a shield immunity strategy depends on many factors, including demographics and interaction context. Beyond the near term, the duration of immune memory is also relevant in projecting to a multi-year post-pandemic framework where demographic dynamics and strain evolution are increasingly relevant^{38,39}. Hence, a serological testing initiative, with repeated testing over time, could benefit intervention efforts while also providing critical information on seroconversion and the risk of re-infection to recovered individuals.

Finally, it will be critical to understand how shield immunity is modulated by spatial and network structure. In a network, well-connected individuals have a disproportionate effect on the spread of disease²². Network structure represents an opportunity to position immune shields at focal points of essential services, and even to prioritize a focus on population-scale serological prevalence assays based on the connectivity of recovered individuals. In the present analysis, we assumed that interactions with recovered individuals occur at a rate $(1+\alpha)$ higher than with other individuals, enabling population-scale shield immunity to emerge before herd immunity. However, there are multiple interaction mechanisms that could yield such interaction substitution, including both ‘flexible’ and ‘fixed’ shielding mechanisms that take different approaches to the extent to which recovered individuals alone, or all individuals, modulate their contact rates. As shown in Extended Data Fig. 1, these mechanisms have the potential to enhance the impact of shielding at lower levels of α . Further studies are needed to explore how these

mechanisms could guide efforts to rewire networked interactions to minimize transmission while also alleviating the impacts of social distancing by partially restoring network connectivity.

Although the number of laboratory-confirmed cases of SARS-CoV-2 is staggering and growing, the actual number of infections is higher—probably far higher. For example, in China, 80% of transmissions of new cases were from undocumented infections²⁸ and there is considerable uncertainty with respect to case ascertainment⁴⁰. Asymptomatic transmission could, paradoxically, provide a greater pool of recovered individuals to develop shield immunity at scale. We contend that it is time for collective action to ascertain more information on outbreak size and to consider the strategic use of serology as the basis for integrative public health interventions to control the pandemic spread of COVID-19.

Online content

Any methods, additional references, Nature Research reporting summaries, source data, extended data, supplementary information, acknowledgements, peer review information; details of author contributions and competing interests; and statements of data and code availability are available at <https://doi.org/10.1038/s41591-020-0895-3>.

Received: 31 March 2020; Accepted: 21 April 2020;

Published online: 07 May 2020

References

- Fauci, A. S., Lane, H. C. & Redfield, R. R. Covid-19—navigating the uncharted. *N. Engl. J. Med.* **382**, 1268–1269 (2020).
- Li, Q. et al. Early transmission dynamics in Wuhan, China, of novel coronavirus-infected pneumonia. *N. Engl. J. Med.* **382**, 1199–1207 (2020).
- Zhou, P. et al. A pneumonia outbreak associated with a new coronavirus of probable bat origin. *Nature* **579**, 270–273 (2020).
- World Health Organization *Coronavirus Disease 2019 (COVID-19) Situation Report 70* (2020); https://www.who.int/docs/default-source/coronavirus/situation-reports/20200409-sitrep-80-covid-19.pdf?sfvrsn=1b685d64_2
- Ferguson, N. et al. *Impact of Non-Pharmaceutical Interventions (NPIs) to Reduce COVID19 Mortality and Healthcare Demand* (Imperial College, 2020); <https://www.imperial.ac.uk/media/imperial-college/medicine/sph/ide/gida-fellowships/Imperial-College-{COVID19}-NPI-modelling-16-03-2020.pdf>
- Amanat, F. et al. A serological assay to detect SARS-CoV-2 seroconversion in humans. Preprint at <https://www.medrxiv.org/content/early/2020/03/18/2020.03.17.20037713> (2020).
- Okba, N. et al. Severe acute respiratory syndrome coronavirus 2-specific antibody responses in coronavirus disease 2019 patients. *Emerg. Infect. Dis.* <https://doi.org/10.3201/eid2607.200841> (2020).
- Zhao, J. et al. Antibody responses to SARS-CoV-2 in patients of novel coronavirus disease 2019. *Clin. Infect. Dis.* <https://doi.org/10.1093/cid/ciaa344> (2020).
- McMichael, T. M. et al. Epidemiology of Covid-19 in a long-term care facility in King County, Washington. *N. Engl. J. Med.* <https://doi.org/10.1056/NEJMoa2005412> (2020).
- Lourenco, J. et al. Fundamental principles of epidemic spread highlight the immediate need for large-scale serological surveys to assess the stage of the SARS-CoV-2 epidemic. Preprint at <https://www.medrxiv.org/content/early/2020/03/26/2020.03.24.20042291> (2020).
- Lipsitch, M., Swerdlow, D. L. & Finelli, L. Defining the epidemiology of Covid-19—studies needed. *N. Engl. J. Med.* **382**, 1194–1196 (2020).
- Chen, L., Xiong, J., Bao, L. & Shi, Y. Convalescent plasma as a potential therapy for COVID-19. *Lancet Infect. Dis.* **20**, 398–400 (2020).
- Duan, K. et al. Effectiveness of convalescent plasma therapy in severe COVID-19 patients. *Proc. Natl Acad. Sci. USA* **117**, 9490–9496 (2020).
- Roback, J. D. & Guarner, J. Convalescent plasma to treat COVID-19: possibilities and challenges. *JAMA* **323**, 1561–1562 (2020).
- National COVID-19 Convalescent Plasma Project (Michigan State University); <https://ccpp19.org/>
- Hennekens, C. H., George, S., Adirim, T. A., Johnson, H. & Maki, D. G. The emerging pandemic of coronavirus: the urgent need for public health leadership. *Am. J. Med.* <https://doi.org/10.1016/j.amjmed.2020.03.001> (2020).
- Chinazzi, M. et al. The effect of travel restrictions on the spread of the 2019 novel coronavirus (COVID-19) outbreak. *Science* **368**, 395–400 (2020).
- Kraemer, M. U. G. et al. The effect of human mobility and control measures on the COVID-19 epidemic in China. *Science* **368**, 493–497 (2020).

19. Flaxman, S. et al. *Report 13: Estimating the Number of Infections and the Impact of Non-Pharmaceutical Interventions on COVID-19 in 11 European Countries* (Imperial College, 2020); <https://spiral.imperial.ac.uk/bitstream/10044/1/77731/9/2020-03-30-COVID19-Report-13.pdf>
20. McKee, M. & Stuckler, D. If the world fails to protect the economy, COVID-19 will damage health not just now but also in the future. *Nat. Med.* <https://doi.org/10.1038/s41591-020-0863-y> (2020).
21. Watts, D. J., Muhamad, R., Medina, D. C. & Dodds, P. S. Multiscale, resurgent epidemics in a hierarchical metapopulation model. *Proc. Natl Acad. Sci. USA* **102**, 11157–11162 (2005).
22. Bansal, S., Grenfell, B. T. & Meyers, L. A. When individual behaviour matters: homogeneous and network models in epidemiology. *J. R. Soc. Interface* **4**, 879–891 (2007).
23. Balcan, D. et al. Multiscale mobility networks and the spatial spreading of infectious diseases. *Proc. Natl Acad. Sci. USA* **106**, 21484–21489 (2009).
24. Colizza, V., Barrat, A., Barthélémy, M. & Vespignani, A. The role of the airline transportation network in the prediction and predictability of global epidemics. *Proc. Natl Acad. Sci. USA* **103**, 2015–2020 (2006).
25. Klompas, M. Coronavirus disease 2019 (COVID-19): protecting hospitals from the invisible. *Ann. Internal Med.* <https://doi.org/10.7326/M20-0751> (2020).
26. Park, S. W., Cornforth, D. M., Dushoff, J. & Weitz, J. S. The time scale of asymptomatic transmission affects estimates of epidemic potential in the COVID-19 outbreak. Preprint at <https://www.medrxiv.org/content/10.1101/2020.03.09.20033514v1> (2020).
27. Wu, J. T., Leung, K. & Leung, G. M. Nowcasting and forecasting the potential domestic and international spread of the 2019-nCoV outbreak originating in Wuhan, China: a modelling study. *Lancet* **395**, 689–697 (2020).
28. Li, R. et al. Substantial undocumented infection facilitates the rapid dissemination of novel coronavirus (SARS-CoV2). *Science* **368**, 489–493 (2020).
29. Wu, J. et al. Estimating clinical severity of COVID-19 from the transmission dynamics in Wuhan, China. *Nat. Med.* **26**, 506–510 (2020).
30. Park, S. W. et al. Reconciling early-outbreak estimates of the basic reproductive number and its uncertainty: framework and applications to the novel coronavirus (SARS-CoV-2) outbreak. Preprint at <https://www.medrxiv.org/content/10.1101/2020.01.30.20019877v4.full.pdf> (2020).
31. Onder, G., Rezza, G. & Brusaferro, S. Case-fatality rate and characteristics of patients dying in relation to COVID-19 in Italy. *JAMA* <https://doi.org/10.1001/jama.2020.4683> (2020).
32. Lou, B. et al. Serology characteristics of SARS-CoV-2 infection since the exposure and post symptoms onset. Preprint at <https://www.medrxiv.org/content/early/2020/03/27/2020.03.23.20041707> (2020).
33. Callow, K., Parry, H., Sergeant, M. & Tyrrell, D. The time course of the immune response to experimental coronavirus infection of man. *Epidemiol. Infect.* **105**, 435–446 (1990).
34. Chan, K.-H. et al. Cross-reactive antibodies in convalescent SARS patients' sera against the emerging novel human coronavirus EMC (2012) by both immunofluorescent and neutralizing antibody tests. *J. Infect.* **67**, 130–140 (2013).
35. Bellan, S. E., Pulliam, J. R., Dushoff, J. & Meyers, L. A. Ebola control: effect of asymptomatic infection and acquired immunity. *Lancet* **384**, 1499–1500 (2014).
36. Emanuel, E. J. We can safely restart the economy in June. Here's how. *New York Times* (28 March 2020); <https://www.nytimes.com/2020/03/28/opinion/coronavirus-economy.html>
37. Gottlieb, S., Rivers, C., McClellan, M., Silvis, L. & Watson, C. *National Coronavirus Response: A Road Map to Reopening* (American Enterprise Institute, 2020); <https://www.aei.org/research-products/report/national-coronavirus-response-a-road-map-to-reopening/>
38. Hadfield, J. et al. Nextstrain: real-time tracking of pathogen evolution. *Bioinformatics* **34**, 4121–4123 (2018).
39. Kissler, S. M., Tedijanto, C., Goldstein, E., Grad, Y. H. & Lipsitch, M. Projecting the transmission dynamics of SARS-CoV-2 through the post-pandemic period. *Science* <https://doi.org/10.1126/science.abb5793> (2020).
40. Verity, R. et al. Estimates of the severity of coronavirus disease 2019: a model-based analysis. *Lancet Infect. Dis.* [https://doi.org/10.1016/S1473-3099\(20\)30243-7](https://doi.org/10.1016/S1473-3099(20)30243-7) (2020).

Publisher's note Springer Nature remains neutral with regard to jurisdictional claims in published maps and institutional affiliations.

© The Author(s), under exclusive licence to Springer Nature America, Inc. 2020

Methods

Shielding mechanisms. *Force of infection.* Consider the force of infection to be the contact rate of susceptible individuals multiplied by the probability that the interactions are with an infectious person multiplied by a probability that the event leads to an infection. Let c_s , c_i and c_r equal the contact rates of susceptible, infectious and recovered individuals, respectively. Hence, the force of infection should be proportional to

$$c_s \left(\frac{c_i I}{c_s S + c_i I + c_r R} \right)$$

in which the weighted average of contacts is $c_0 = c_s S + c_i I + c_r R$. When $c_s = c_i = c_0$ and $c_r = c_0(1+\alpha)$, the force of infection is proportional to

$$c_0 \left(\frac{I}{1 + \alpha R} \right)$$

This is the basis for the core shielding model presented in the main text. We consider 'flexible' and 'fixed' shielding mechanisms, which keep the weighted average constant throughout the dynamics.

Flexible shielding. In a flexible shielding mechanism, recovered individuals have $(1+\alpha)$ greater contact rates than susceptible or infectious individuals. Denoting c_b as the baseline contact rate of susceptible and infectious individuals (equal to both c_s and c_i) implies that $c_r = (1+\alpha)c_b$. Hence, for flexible shielding the weighted average becomes

$$c_b(S + I) + c_b(1 + \alpha)R = c_0$$

or equivalently

$$c_b(1 - R) + c_b(1 + \alpha)R = c_0$$

such that

$$c_b = \frac{c_0}{1 - R + R + \alpha R} = \frac{c_0}{1 + \alpha R}$$

As a result, the force of infection is proportional to

$$\frac{c_b^2 I}{c_0}$$

or

$$\frac{c_0 I}{(1 + \alpha R)^2}$$

The resulting SIR dynamics with flexible shielding are

$$\begin{aligned} \dot{S} &= -\beta \frac{SI}{(1+\alpha R)^2} \\ \dot{I} &= \beta \frac{SI}{(1+\alpha R)^2} - \gamma I \\ \dot{R} &= \gamma I \end{aligned}$$

Flexible shielding has an even stronger effect on epidemic outbreaks than analysis of the core shielding model ($1/(1 + \alpha R)$) presented in the main text (Extended Data Fig. 1). In keeping the number of contacts constant, infectious and susceptible individuals diminish their interactions given more shields to replace them.

Fixed shielding. In a fixed shielding mechanism, recovered individuals have $(1+\alpha)$ greater contact rates relative to their original baseline, such that the new weighted average is

$$c_b(1 - R) + c_0(1 + \alpha)R = c_0$$

implying

$$c_b = c_0 \frac{1 - (1 + \alpha)R}{1 - R}$$

Hence, the force of infection is proportional to

$$\frac{c_b^2 I}{c_0}$$

or

$$\frac{c_0(1 - (1 + \alpha)R)^2}{(1 - R)^2} I$$

The resulting SIR dynamics with fixed shielding are

$$\begin{aligned} \dot{S} &= -\beta \frac{SI(1 - (1 + \alpha)R)^2}{(1 - R)^2} \\ \dot{I} &= \beta \frac{SI(1 - (1 + \alpha)R)^2}{(1 - R)^2} - \gamma I \\ \dot{R} &= \gamma I \end{aligned}$$

This model is applicable insofar as $(1 + \alpha)R \leq 1$, such that the epidemic must have an outbreak size $R_\infty \leq 1/(1 + \alpha)$. Like flexible shielding, the fixed shielding mechanism also outperforms the core shielding model presented in the main text (Extended Data Fig. 1).

Assumptions for an age-structured model. Consider a population of susceptible (S), exposed (E), infectious asymptomatic (I_{asym}), infectious symptomatic (I_{sym}) and recovered (R) who are free to move, without restrictions in a 'business as usual' scenario. A subset of symptomatic cases will require hospital care, which we further divide into subacute (I_{hsub}) and critical/acute (that is, requiring ICU intervention, I_{hcrit}) cases. Vital dynamics (births and other causes of death) are ignored for simplicity. The model is visually represented in Extended Data Fig. 2 and the system of nonlinear differential equations governing this age-structured epidemiological model are as follows:

$$\begin{aligned} \frac{dS(a)}{dt} &= \underbrace{-\beta_s S(a) I_{\text{sym,tot}}}_{\text{symptomatic contact}} - \underbrace{\beta_a S(a) I_{\text{asym,tot}}}_{\text{asymptomatic contact}} \quad \text{onset of infectiousness} \\ \frac{dE(a)}{dt} &= \underbrace{\beta_s S(a) I_{\text{sym,tot}}}_{\text{symptomatic contact}} + \underbrace{\beta_a S(a) I_{\text{asym,tot}}}_{\text{asymptomatic contact}} - \underbrace{\gamma_e E(a)}_{\text{recovery}} \\ \frac{dI_{\text{sym}}(a)}{dt} &= \underbrace{p(a) \gamma_e E(a)}_{\text{symptomatic onset}} - \underbrace{\gamma_a I_{\text{sym}}(a)}_{\text{transfer from } I_{\text{sym}}} \\ \frac{dI_{\text{asym}}(a)}{dt} &= \underbrace{(1 - p(a)) \gamma_e E(a)}_{\text{subcritical cases}} - \underbrace{\gamma_s I_{\text{sym}}(a)}_{\text{transfer from } I_{\text{hsub}}} \\ \frac{dI_{\text{hsub}}(a)}{dt} &= \underbrace{h(a)(1 - \xi(a)) \gamma_s I_{\text{sym}}(a)}_{\text{critical (ICU) cases}} - \underbrace{\gamma_h I_{\text{hsub}}(a)}_{\text{transfer from } I_{\text{hcrit}}} \\ \frac{dI_{\text{hcrit}}(a)}{dt} &= \underbrace{h(a)\xi(a) \gamma_s I_{\text{sym}}(a)}_{\text{recovery from } I_{\text{asym}}} - \underbrace{\gamma_h I_{\text{hcrit}}(a)}_{\text{recovery from } I_{\text{sym}}} \quad \text{recovery from } I_{\text{hsub}} \quad \text{recovery from } I_{\text{hcrit}} \\ \frac{dR(a)}{dt} &= \underbrace{\gamma_a I_{\text{sym}}(a)}_{\text{mortality}} + \underbrace{(1 - h(a)) \gamma_s I_{\text{sym}}(a)}_{\text{recovery from } I_{\text{asym}}} + \underbrace{\gamma_h I_{\text{hsub}}(a)}_{\text{recovery from } I_{\text{hcrit}}} + \underbrace{(1 - \mu) \gamma_h I_{\text{hcrit}}(a)}_{\text{recovery from } I_{\text{hcrit}}} \\ \frac{dD(a)}{dt} &= \mu \gamma_h I_{\text{hcrit}}(a) \end{aligned}$$

where $I_{\text{sym,tot}}$ represents the total number (across all age classes) of symptomatic infectious individuals, $I_{\text{asym,tot}}$ the total number of asymptomatic infectious individuals, N_{tot} the total number of circulating individuals and R_{shields} the number of recovered individuals who could serve as serological shields (which we define as those of ages between 20 and 59 years), given age classes a . The assumed model parameters used in the baseline models are presented in Supplementary Tables 1 and 2.

Varying the intensity of the outbreak \mathcal{R}_0 . Based on the parameters in Supplementary Tables 1 and 2, \mathcal{R}_0 is calculated as a weighted average between the symptomatic and asymptomatic reproduction numbers, $\mathcal{R}_{\text{asym}}$ and \mathcal{R}_{sym} , respectively:

$$\mathcal{R}_0 = p \mathcal{R}_{\text{asym}} + (1 - p) \mathcal{R}_{\text{sym}}$$

These can be further expanded based on age group to obtain

$$\mathcal{R}_0 = \sum_{a \in \text{Age Groups}} p(a) f_a \mathcal{R}_{\text{asym}}(a) + (1 - p(a)) f_a \mathcal{R}_{\text{sym}}(a)$$

where f_a denotes the fraction of individuals in age class a , which yields a basic reproduction number of ~ 1.57 in the low scenario and 2.33 in the high scenario.

Initial conditions in the extended model. The baseline model assumes a population of 10,000,000 with age demographics as given in Supplementary Table 2 unless stated otherwise. An initial outbreak is seeded in this population given one exposed individual in the 20–29 years age class. The simulation is run forward until 10,000 people have been exposed to the virus (that is, 10,000 people are no longer in the susceptible states). We use this time point (which we denote time 0 in our simulations) as the time at which intervention policies might be applied. At this point, once 10,000 people have already been exposed, we simulate the dynamics forward either with or without the interventions.

Interaction substitution and demography. Demography has potential impacts on the spread and consequences of coronavirus and on the efficacy of intervention strategies. We evaluated the baseline model and shielding scenarios $\alpha=2$ and $\alpha=20$ given the age structure for the United States, that is, including 50 states, Washington DC and Puerto Rico. The states include significant variation in the fraction of the population that is over 60 years, ranging from less than 16% (Utah)

to above 28% (Maine). We observe a demographic dependence on the efficacy of shielding for both per capita cumulative deaths and per capita peak ICU demand, linked to the fraction of the population that is 60 years and above. The relationship is linear under both the low and high \mathcal{R}_0 scenarios (Extended Data Fig. 3). Outcomes are better when the population has more younger individuals (given that age-stratified risk will favor improved outcomes for those who are infected). However, notably, shielding reduces the difference in outcomes; for example, whereas the cumulative deaths for Utah are 440 (400) less per 100,000 than Maine in the baseline case, they are only 210 (120) less per 100,000 than Maine in the $\alpha=20$ shielding case for the high (low) \mathcal{R}_0 scenarios. Hence, demographic distributions that are relatively older will favor deployment of shields (in a relative sense). We note that, although we have treated state-level demographics uniformly, this result also points toward the benefits of shield immunity in areas with right-shifted age distributions as potential targets for intervention, with potential consequences for deployment of shields in other countries with right-shifted demographics (for example, Italy).

Variation with asymptomatic cases. We investigated the impact of asymptomatic transmission on the efficacy of immune shielding as an intervention. First, we fixed the intrinsic asymptomatic fraction p from 0.5 to 0.95 for scenarios corresponding to $\alpha=0, 2$ and 20 (Extended Data Fig. 4). Irrespective of the shielding preference α , increases in p reduce total deaths and ICU cases by ~90% when \mathcal{R}_0 is constant and more than 90% when \mathcal{R}_0 is a function of p , given variation from $p=0.5$ to $p=0.95$. We observed that the impact of immune shielding is higher at low p . Second, we considered the effects of age-dependent variation in the intrinsic asymptomatic fraction, $p(a)$, by fixing the average p at 0.5, 0.75 and 0.9, given observations of increasing risk based on clinical outcome data from Wuhan, China²⁹ (Extended Data Fig. 5). The impact of immune shielding is robust to observed age-specific variation p , that is, leading to significant decreases of projected deaths and ICU cases (Extended Data Fig. 6).

Impacts of waning immunity. We extended the core model to account for potential impacts of waning immunity by including explicit state-structured shield compartments consisting of newly recruited recovered individuals (H_1) and late-stage recovered individuals that can revert to become susceptible (H_2). In effect, the immunity duration was assumed to be gamma-distributed, after which recovered individuals become susceptible. This is a conservative assumption, given that individuals who lose immunity are likely to have less severe illness if re-infected (but could still pass on an infection to immunologically naive individuals). Extended Data Fig. 7 shows the outbreak dynamics for the high and low \mathcal{R}_0 scenarios with an average immunity duration of two months. Immune shielding can still significantly reduce the number of deaths and the peak number of ICU beds needed for both scenarios, especially for the strong shielding case ($\alpha=20$). In Extended Data Fig. 8, we systematically explore how the cumulative deaths, maximum ICU beds needed and total number of cases depend on the immunity duration. The results show that the efficacy of immune shielding is robust to the duration of immunity, insofar as the duration of immunity persists on the order of multiple months (and not multiple weeks).

Optimized age-dependent immune shielding deployment. In the previous sections, we have assumed that shields (recovered individuals aged 20–59 years) were deployed such that they interact with people of all ages equally. In other words, all the susceptible individuals (across ages) have an infection rate that scales with $I_{\text{tot}}/(N_{\text{tot}} + \alpha R_{\text{shields}})$ such that the shields are uniformly interacting with all ages. In this section, we explore the outcome of having the shields act in positions where they could be more or less likely to interact with different age groups, that is, using the same effort as in the core model, then taking the $\alpha R_{\text{shields}}$ of effort but distributing it non-uniformly across ages. To explore the ‘optimized’ distributions of the shields effort, we introduce non-uniform shield interactions in the model. To do so, we modify the equations of $S(a)$ and $E(a)$ in the core model as follows:

$$\begin{aligned} \frac{dS(a)}{dt} &= -\beta_a \frac{S(a)I_{\text{asym,tot}}}{N_{\text{tot}} + \alpha R_{\text{shields}}(\theta_a/f_a)} - \beta_s \frac{S(a)I_{\text{sym,tot}}}{N_{\text{tot}} + \alpha R_{\text{shields}}(\theta_a/f_a)} \\ \frac{dE(a)}{dt} &= \beta_a \frac{S(a)I_{\text{asym,tot}}}{N_{\text{tot}} + \alpha R_{\text{shields}}(\theta_a/f_a)} + \beta_s \frac{S(a)I_{\text{sym,tot}}}{N_{\text{tot}} + \alpha R_{\text{shields}}(\theta_a/f_a)} - \gamma_e E(a) \end{aligned}$$

where f_a is the fraction of the population of age a (f_a are fixed parameters) and θ_a is the distributed shielding fraction of the subpopulation class of age a , which is how we distribute the shields to interact across different age classes (θ_a are the optimization variables). In addition, we define the ratio θ_a/f_a as the age-dependent shielding concentration. When $f_a/\theta_a = 1$ for all ages a , the uniform shields interactions case is recovered; that is, we recover the core model. We note that $\sum_a \theta_a = 1$, such that the effort is the same as in the core model, but allowing for asymmetric distribution across ages. For example, if 25% of the population has age a and receives 100% of the shield protection, then $f_a = 0.25$ and $\theta_a = 1$; this implies $\theta_a/f_a = 4$, that is, a fourfold boosted protection for that particular class.

The optimization objective is to minimize total deaths $D_{\text{tot}}(t_f)$, where t_f is the final time of the simulation—one year after shielding begins, while keeping ICU beds less than the maximum carrying capacity B at every time instant. We seek to find the optimum distribution for deploying the effort of the serological

shields. The non-uniform shielding fraction can be represented by a vector $\Theta = [\theta_1, \dots, \theta_{10}]$, and we aim to solve the following minimization problem:

$$\begin{aligned} \min \mathcal{J}(\Theta) &= \int_{t_0}^{t_f} \overbrace{W_i \times d(I_{\text{hcrit}}^{\text{tot}}(t))}^{\text{barrier function (constraint)}} dt + \overbrace{W_d \times D_{\text{tot}}(t_f)}^{\text{costs of deaths}} \\ \text{subject to } &\sum_{a=1}^{10} \theta_a = 1, \quad \theta_a \geq 0 \quad \forall a = 1, 2, \dots, 10; \end{aligned}$$

where W_i and W_d are weight regulators for infections that require hospitalization and for deaths, respectively. The barrier function d is chosen such that it increases the cost dramatically as the number of ICU beds in use approaches the capacity B of the system, to prevent overloading the healthcare system. To satisfy this property, we pick $d(x) = \log(\frac{1}{B-x})$. The barrier function goes to infinity as x approaches B from the left. Here, we consider the maximum capacity B as a ‘strict’ (or ‘hard’) constraint and any distributed shielding fraction Θ that leads to the ICU beds exceeding B is not considered a feasible shielding deployment. Given the simulation results shown in the main text, we set B as 200 ICU beds per 100,000 for the high scenario case and $B=80$ ICU beds per 100,000 people for the low scenario case.

The optimization approach allows us to evaluate if it is possible to improve the effectiveness of serological shields by deploying them unevenly across a population. Moreover, the barrier function in the cost function is negative if $I_{\text{hcrit}}(t) < B - 1$, which is a ‘reward’ if occupancy of the ICU beds is low. In practice, we set W_i to be arbitrarily small because it serves much like a constraint, for example, $W_i = 10^{-7}$. We set $W_d = 1$ as minimizing deaths is the primary goal. The optimization problem is solved via a genetic algorithm⁴¹ using MATLAB’s built-in optimization function ga, with the maximum generation number (set to 30) serving as the stopping criterion⁴².

Extended Data Fig. 9 shows that an improved way of distributing shielding effort is to prioritize low, but non-zero, shielding of young and place increasing effort on shielding elderly members of the population (see Extended Data Fig. 10 for shielding concentrations). Using the optimized shielding deployment, the reduction in deaths ($D_{\text{tot}}(t_f)$) is substantial (~30%). The results suggest advantages of preferentially shielding those who are most at risk.

Reporting Summary. Further information on research design is available in the Nature Research Reporting Summary linked to this article.

Data availability

Population demographics for US states were obtained from the publicly available United States Census Bureau for the year 2018⁴³.

Code availability

All simulation and figure codes used in the creation of this manuscript are available at https://github.com/WeitzGroup/covid_shield_immunity. The core model and extensions to consider the variation of asymptomatic to symptomatic cases, the impact of dual intervention of social distancing and serological shielding, the effects of waning immunity and age-dependent deployment of shields were simulated using MATLAB. Model simulations were numerically integrated using ODE45^{44,45} in MATLAB R2019a. The core model was reproduced in Julia⁴⁶, and extended to look at the effect of different age demographics on disease severity and intervention efficacy. Epidemiological simulations were performed using a 4/5 Runge–Kutta method⁴⁷ implemented in the DifferentialEquations.jl package⁴⁸. The core model was reproduced in R. Simulations were performed in R using the ode45 method⁴⁴ in the deSolve package⁴⁹.

References

41. Whitley, D. A genetic algorithm tutorial. *Stat. Comput.* **4**, 65–85 (1994).
42. Global Optimization Toolbox (MathWorks, 2020).
43. Annual Estimates of the Resident Population by Single Year of Age and Sex: April 1, 2010 to July 1, 2018 (US Census Bureau); https://www2.census.gov/programs-surveys/popest/tables/2010-2018/state/asrh/PEP_2018_PEPSYASEX.zip (accessed 1 May 2020).
44. Dormand, J. R. & Prince, P. J. A family of embedded Runge–Kutta formulae. *J. Comput. Appl. Math.* **6**, 19–26 (1980).
45. Shampine, L. F. & Reichelt, M. W. The MATLAB ODE suite. *SIAM J. Sci. Comput.* **18**, 1–22 (1997).
46. Bezanson, J., Edelman, A., Karpinski, S. & Shah, V. B. Julia: a fresh approach to numerical computing. *SIAM Rev.* **59**, 65–98 (2017).
47. Tsitouras, C. Runge–Kutta pairs of order 5 (4) satisfying only the first column simplifying assumption. *Comput. Math. Applications* **62**, 770–775 (2011).
48. Rackauckas, C. & Nie, Q. DifferentialEquations.jl-a performant and feature-rich ecosystem for solving differential equations in Julia. *J. Open Res. Softw.* **5**, 15 (2017).
49. Soetaert, K. E., Petzoldt, T. & Setzer, R. W. Solving differential equations in R: package deSolve. *J. Stat. Softw.* **33**, 1–28 (2010).

Acknowledgements

We thank P.S. Dodds, M. Lipsitch, K. Levy, D. Muratore, A. Sanz and J. Shaman for comments and feedback in the initial stages of development, and A. Kraay, B. Lopman and K. Nelson for discussions on serological testing characteristics as part of ongoing collaborative work. Tweet threads by T. Bedford and N. Christakis were influential in refining initial ideas into the current form. Research effort by J.S.W. and co-authors at the Georgia Institute of Technology was enabled by support from grants from the Simons Foundation (SCOPE Award ID 329108), the Army Research Office (W911NF1910384), the National Institutes of Health (1R01AI46592-01) and the National Science Foundation (1806606 and 1829636). J.D. was supported in part by grants from the Canadian Institutes of Health Research and the Natural Sciences and Engineering Research Council of Canada.

Author contributions

J.S.W. designed the study, provided oversight for all aspects of the study, developed the core modeling framework, developed simulation code, analyzed models and wrote the manuscript. S.J.B., A.R.C., D.D., M.D.-M., C.-Y.L., G.L., A.M., R.R.-G., S.S. and C.Z. developed simulation code, extended model simulations, analyzed models and

contributed to writing the manuscript. S.W.P. and J.D. contributed to study design, model development and writing the manuscript.

Competing interests

The authors declare no competing interests.

Additional information

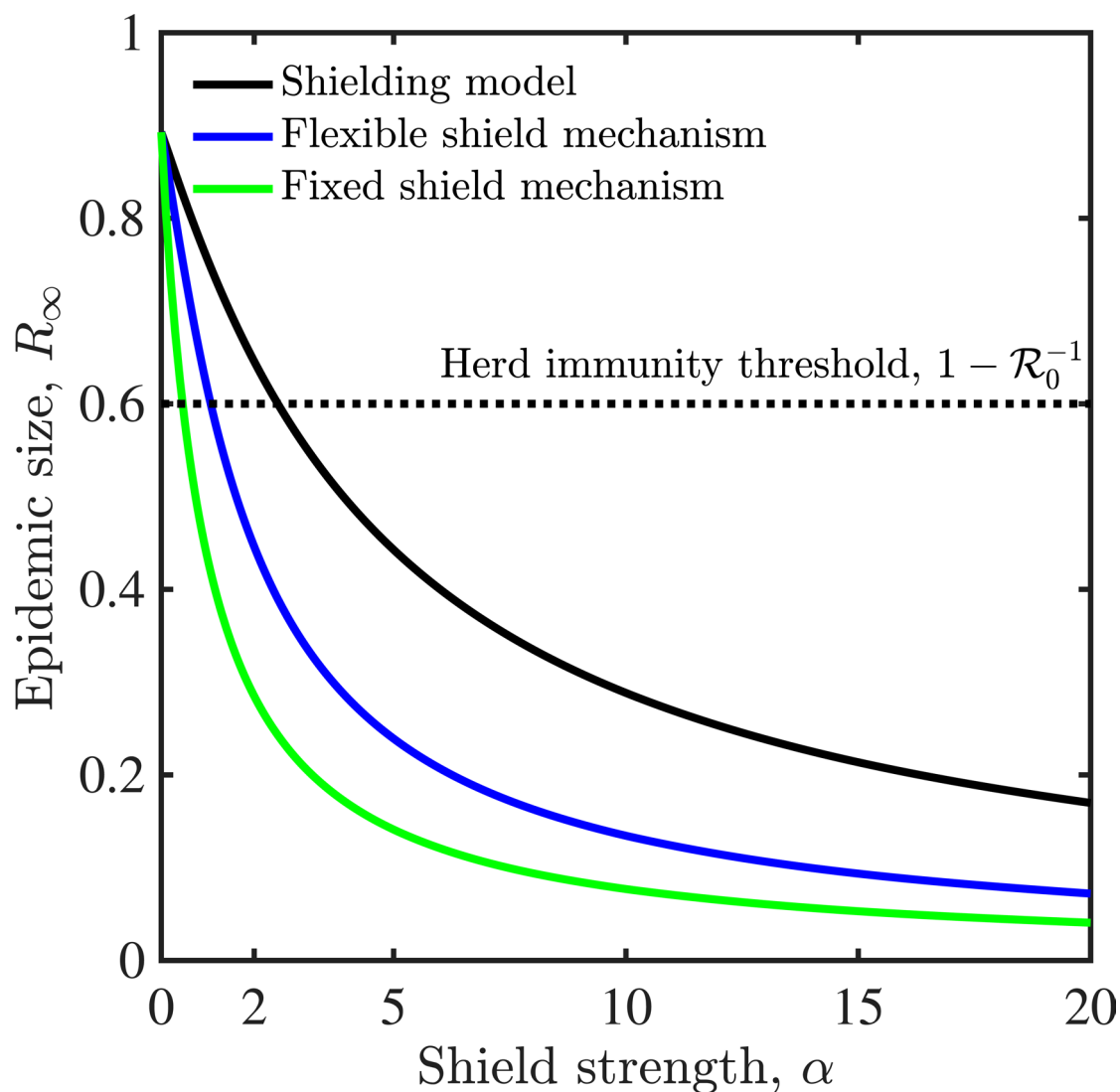
Extended data is available for this paper at <https://doi.org/10.1038/s41591-020-0895-3>.

Supplementary information is available for this paper at <https://doi.org/10.1038/s41591-020-0895-3>.

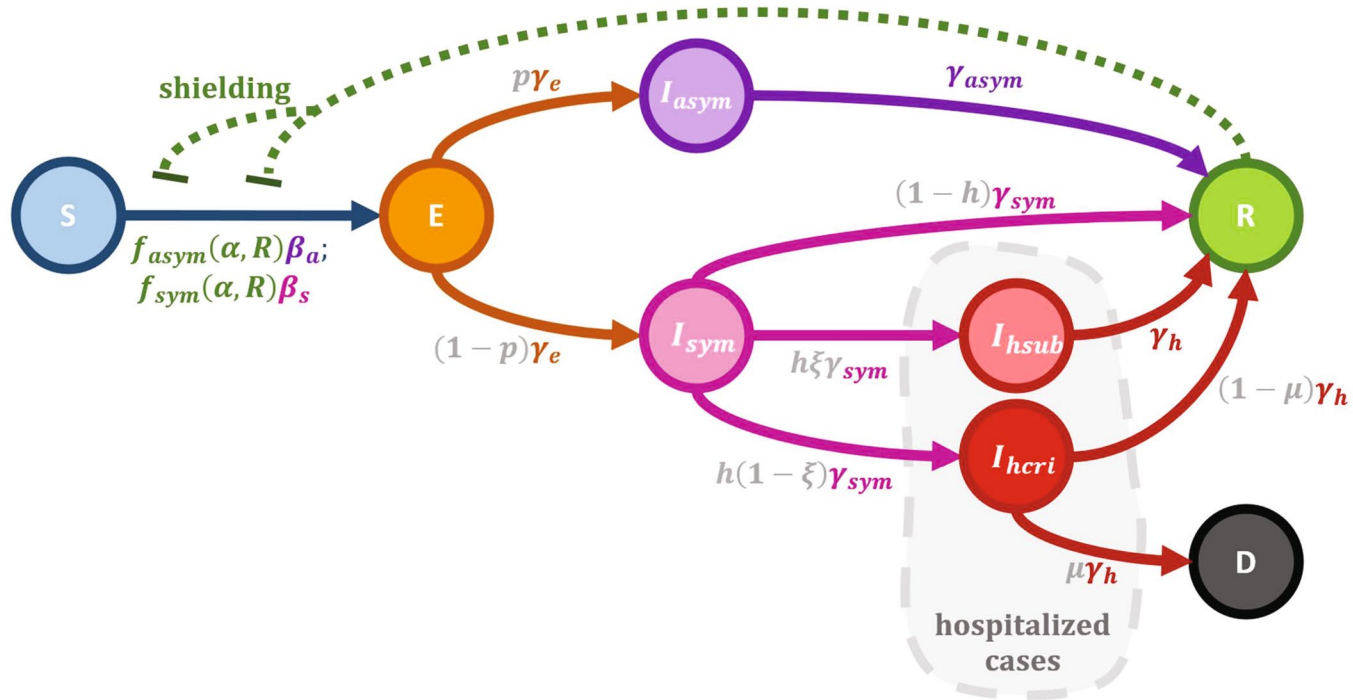
Correspondence and requests for materials should be addressed to J.S.W.

Peer review information Jennifer Sargent was the primary editor on this article and managed its editorial process and peer review in collaboration with the rest of the editorial team.

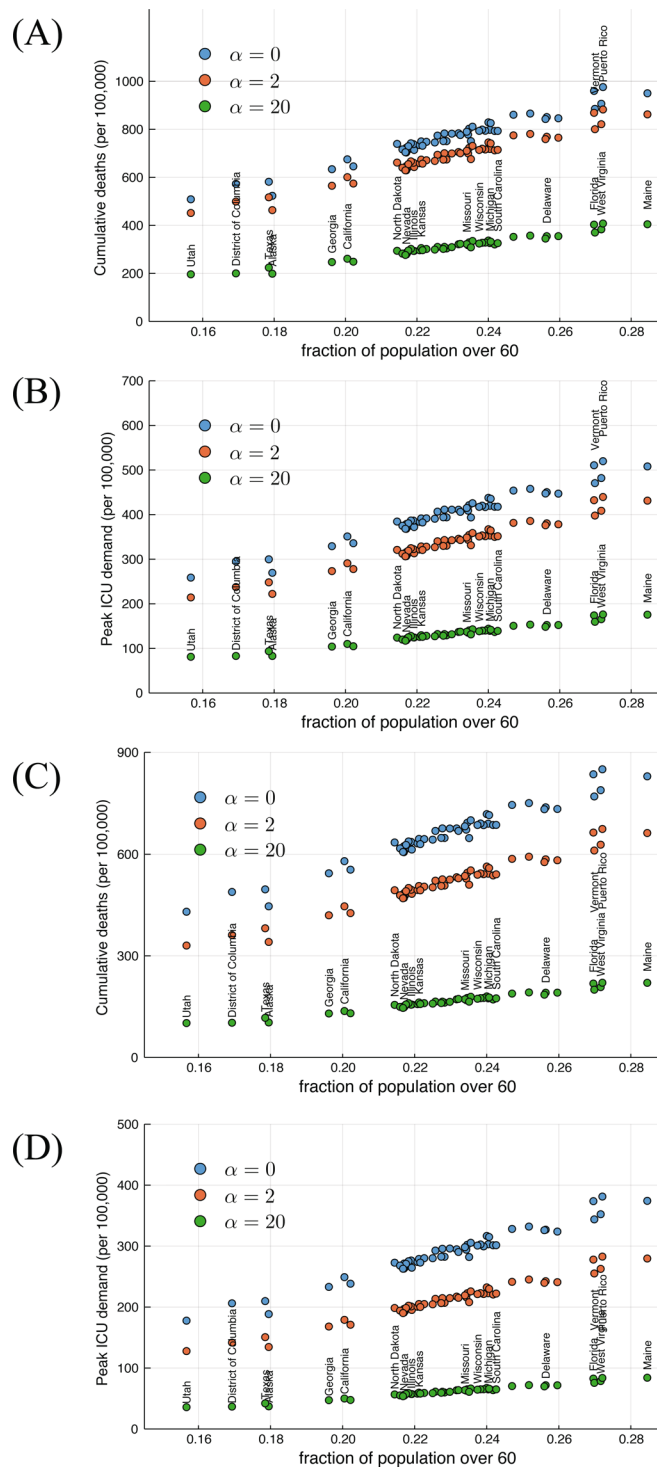
Reprints and permissions information is available at www.nature.com/reprints.



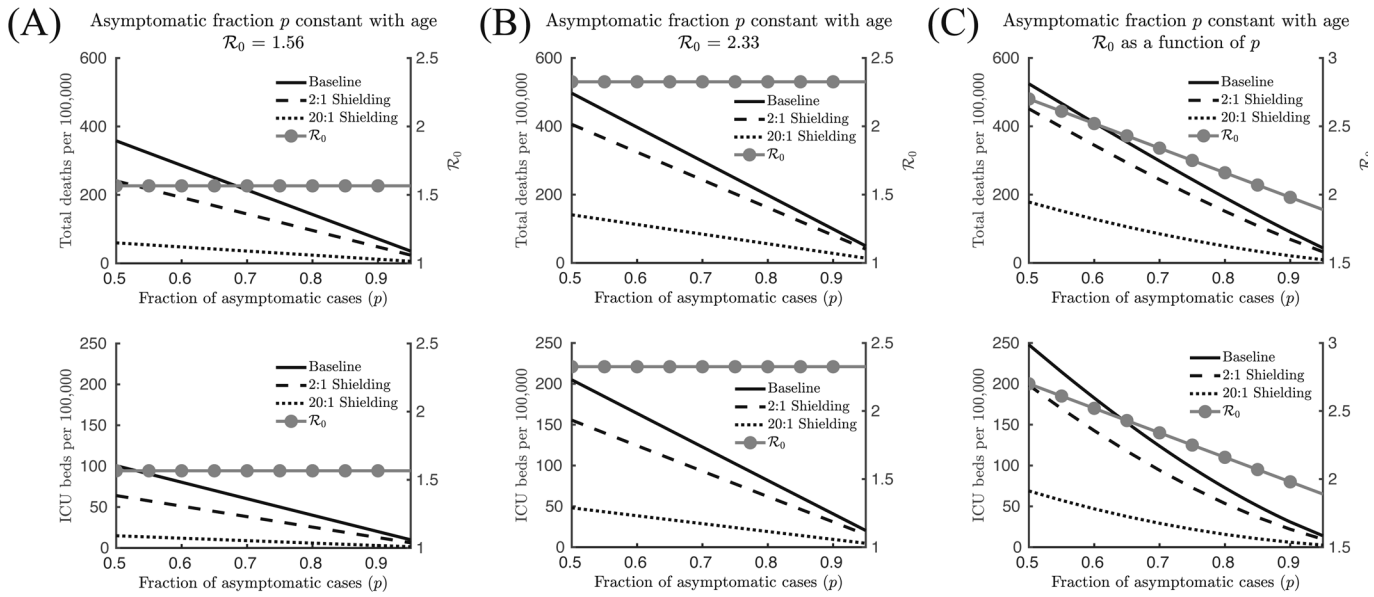
Extended Data Fig. 1 | Impact of shielding mechanisms on final size outcomes in a SIR model. In each case, the epidemic size is plotted (on the y-axis) against the shielding strength, α (x-axis) given $\mathcal{R}_0=2.5$. The three curves denote shielding of recovered individuals by a factor of $1 + \alpha$ (black) as described in the main text, a ‘flexible’ shielding mechanism where the total contact rate is constrained, but recovered individuals vary in their contact rates during the epidemic, and a ‘fixed’ shielding mechanism where the total contact rate is constrained, but recovered individuals have fixed contact rates during the epidemic. See Methods for details.



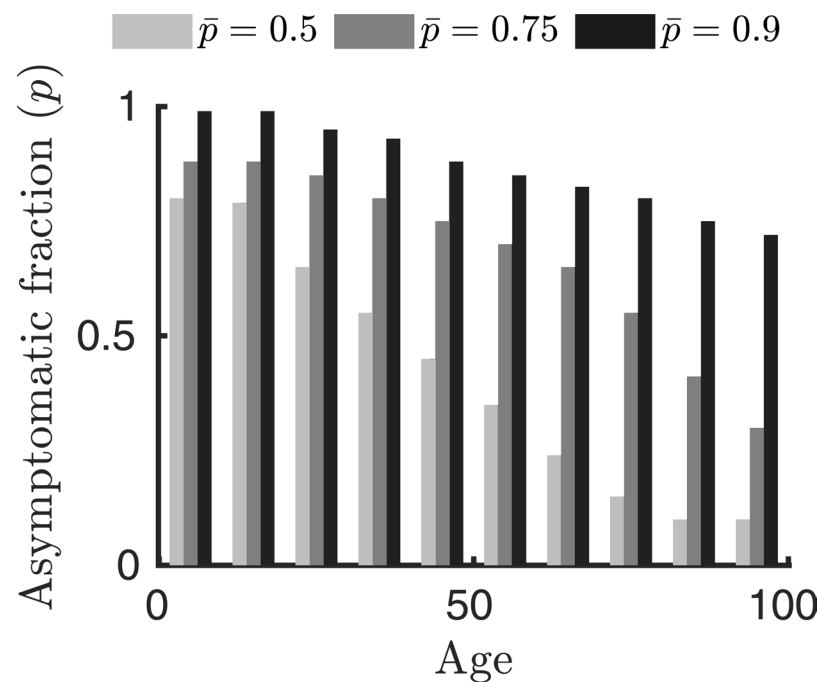
Extended Data Fig. 2 | Model schematic. We consider a population susceptible individuals (S), interacting with infected (I_{sym} , I_{asym}) and recovered (R) individuals. Interactions between susceptible and infectious individuals lead to new exposed cases (E). Exposed individuals undergo a period of latency before disease onset, which are symptomatic (I_{sym}) or asymptomatic (I_{asym}). A subset of symptomatic individuals require hospitalization (I_h) which we further categorize as acute/subcritical (I_{hsub}) and critical (I_{hcri}) cases, the latter of which can be fatal. Individuals who recover can then mitigate the rate of new exposure cases by interaction substitution - what we denote as *immune shielding* - by modulating the rate of susceptible-infectious interactions by $f_{asym}(\alpha, R)$ and $f_{sym}(\alpha, R)$ respectively, where $f_{asym}(\alpha, R) = \frac{S(a)I_{asym,tot}}{N_{tot} + \alpha R_{shields}}$. Here, the tot subscript denotes the total number of cases across all ages, that is $I_{sym,tot} = \sum_a I_{sym}(a)$.



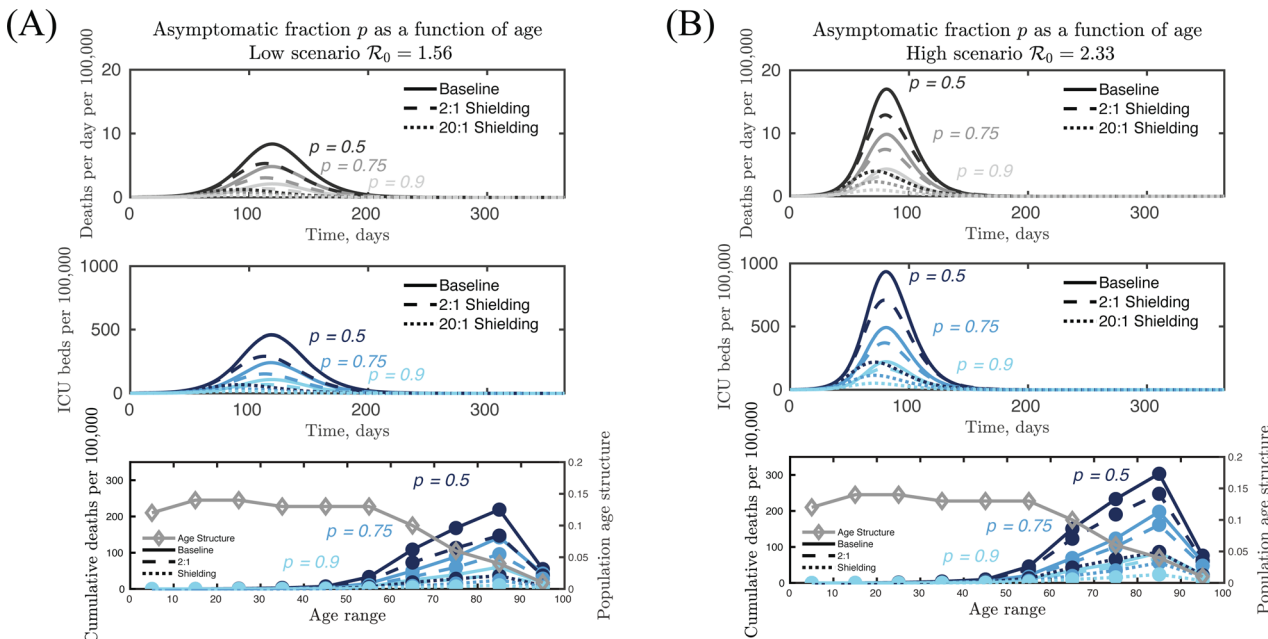
Extended Data Fig. 3 | Impact of demography on the intervention benefits of immune shielding. Panels depict a high (**a, b**) and low (**c, d**) \mathcal{R}_0 scenario. States are ordered by fraction of population above 60 (x-axis) with the baseline, low and high shielding scenarios shown; labels of some but not all states are shown for clarity.



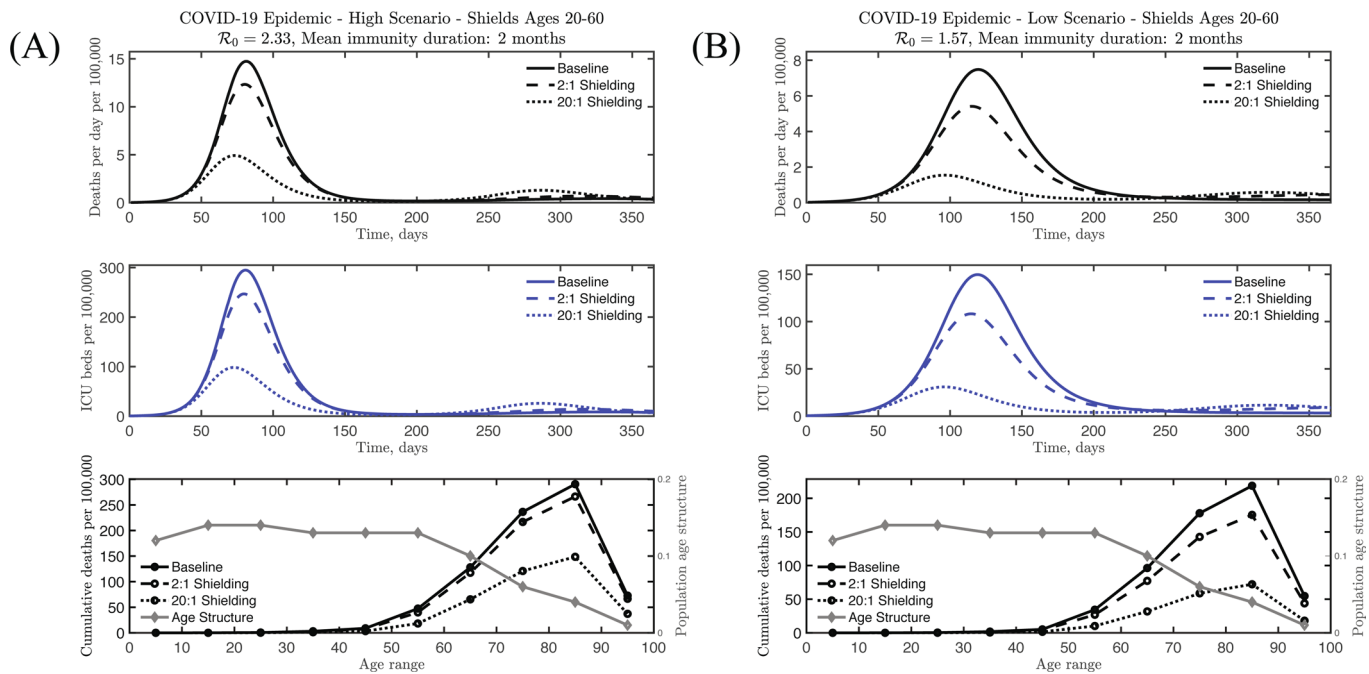
Extended Data Fig. 4 | Impact of asymptomatic fraction and shielding on the total deaths and the peak ICU cases. Panels depict a constant \mathcal{R}_0 (low scenario panel **a**, high scenario panel **b**) and a dynamic \mathcal{R}_0 (panel **c**). The fraction of asymptomatic p is the same for all ages in the three panels. Shielding offers improvement to outcomes, particularly at lower asymptomatic fractions.



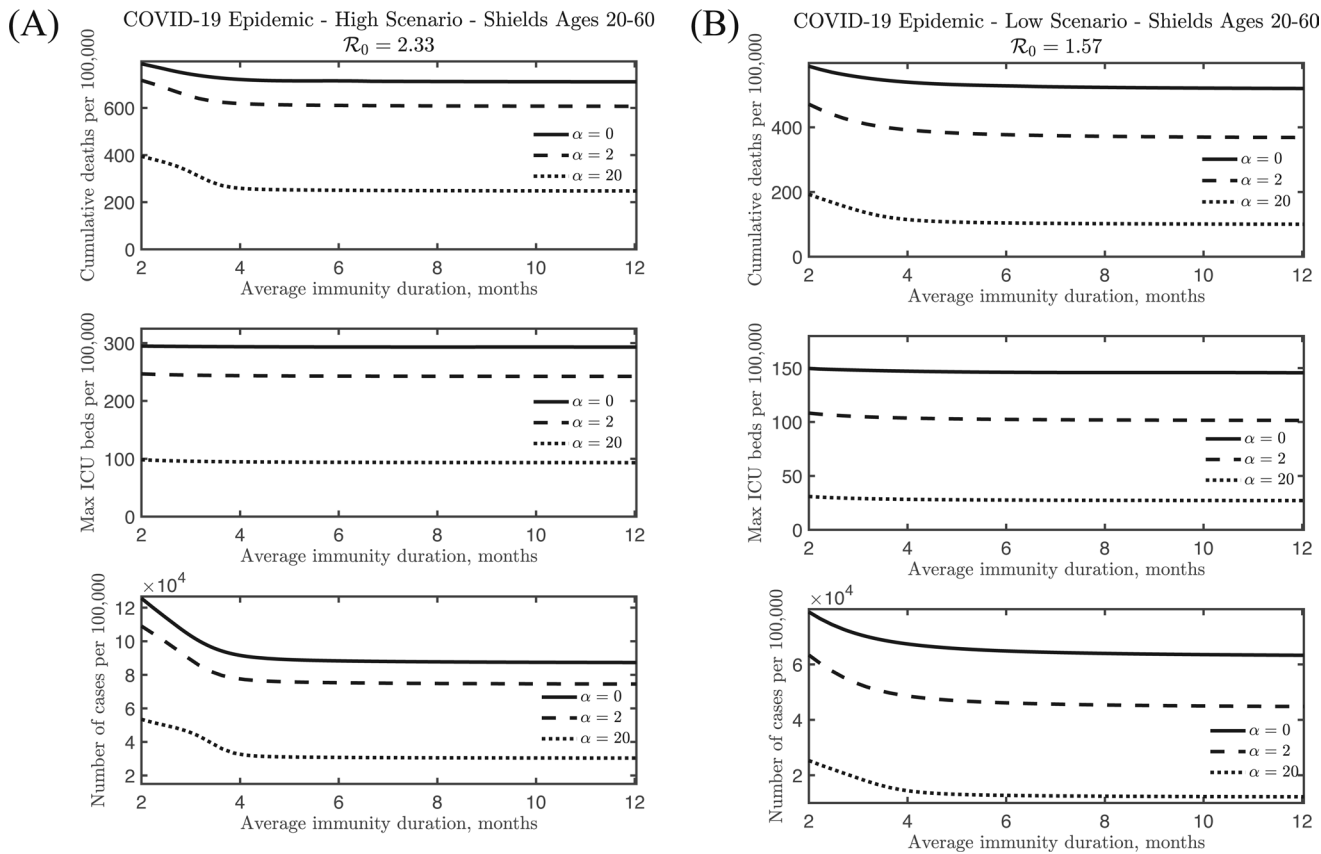
Extended Data Fig. 5 | Age distribution assumptions of the asymptomatic fraction. The profiles of p correspond to three different average p : $\bar{p} = 0.5$, $\bar{p} = 0.75$, and $\bar{p} = 0.9$.



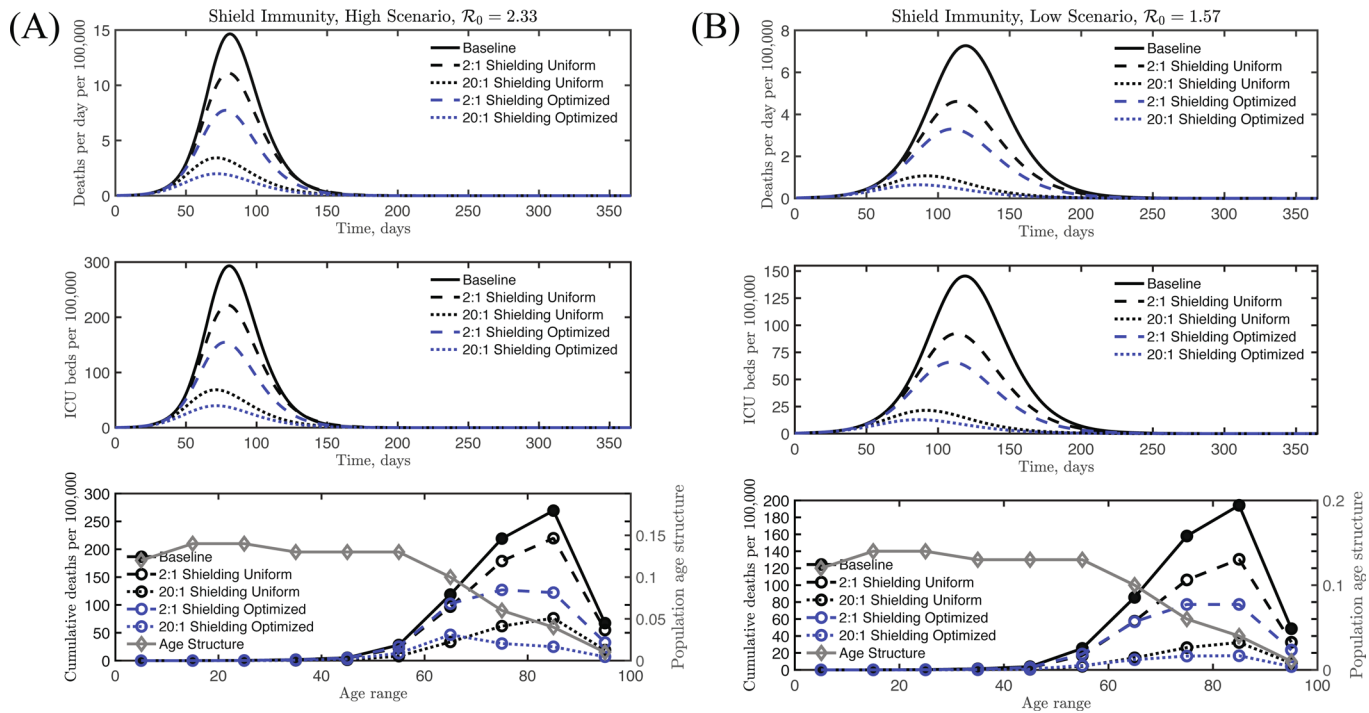
Extended Data Fig. 6 | COVID-19 dynamics in a baseline case without interventions compared to two shielding scenarios and three asymptomatic fraction cases. The shield scenarios ($\alpha=0$ and $\alpha=20$) and three age-distributed asymptomatic fraction values ($\bar{p} = 0.5$, $\bar{p} = 0.75$ and $\bar{p} = 0.9$) are evaluated for both a high scenario ($\mathcal{R}_0 = 2.33$ - panel **a**) and low scenario ($\mathcal{R}_0 = 1.57$, panel **b**). The impact of immune shielding is robust to observed age-specific variation p , that is, leading to significant decreases of projected deaths and ICU cases.



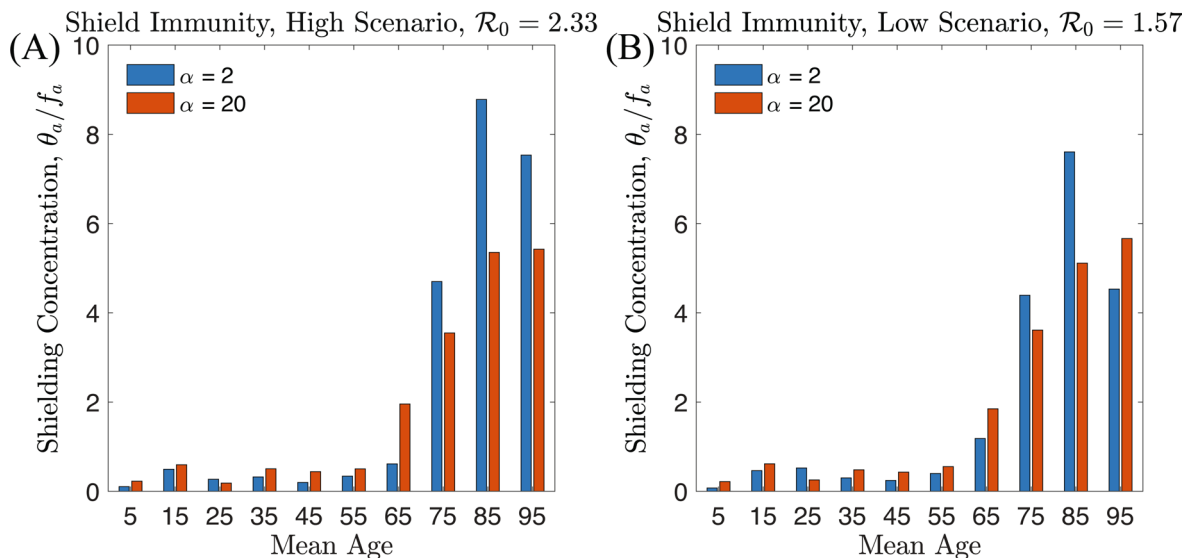
Extended Data Fig. 7 | COVID-19 dynamics given variation in immune duration. Panels denote simulations with high (**a**) and low (**b**) \mathcal{R}_0 scenarios. We compared a baseline case without interventions to two shielding scenarios ($\alpha=2$ and $\alpha=20$) with a mean immunity duration of 2 months. Immune shielding can still significantly reduce the number of deaths and ICU beds needed for a finite immunity duration.



Extended Data Fig. 8 | Comparing the effectiveness of shielding given variation in immunity duration. Simulations correspond to high (a) and low (b) \mathcal{R}_0 scenarios. Shielding is effective at reducing epidemic burden compared to the baseline with no shielding for a wide range of immunity duration. When immunity lasts approximately 4 months or less, re-infection of recovered individuals leads to an increase in the number of deaths and total cases.



Extended Data Fig. 9 | COVID-19 dynamics given optimized age-dependent shield deployment. Simulations in the two shielding scenarios ($\alpha=2$ and $\alpha=20$) are compared to the scenarios with optimized age-dependent shield deployment for the same values of α with the baseline case included for reference. The results are displayed for both high (a) and low (b) \mathcal{R}_0 scenarios. The optimal deployment significantly reduces the total death count and the need for ICU beds for both $\alpha=2$ and $\alpha=20$.



Extended Data Fig. 10 | Optimal shielding concentration for all age classes. Panels denote high (A) and low (B) \mathcal{R}_0 scenarios. The optimal shielding concentrations (for both scenarios) are obtained via solving an optimization problem with low and high shielding levels (see Methods). The optimal shielding concentration (θ_a/f_a) is larger for classes with a higher age, which would reduce casualties as the older population is disproportionately affected by COVID-19.

Reporting Summary

Nature Research wishes to improve the reproducibility of the work that we publish. This form provides structure for consistency and transparency in reporting. For further information on Nature Research policies, see [Authors & Referees](#) and the [Editorial Policy Checklist](#).

Statistics

For all statistical analyses, confirm that the following items are present in the figure legend, table legend, main text, or Methods section.

n/a Confirmed

- The exact sample size (n) for each experimental group/condition, given as a discrete number and unit of measurement
- A statement on whether measurements were taken from distinct samples or whether the same sample was measured repeatedly
- The statistical test(s) used AND whether they are one- or two-sided
Only common tests should be described solely by name; describe more complex techniques in the Methods section.
- A description of all covariates tested
- A description of any assumptions or corrections, such as tests of normality and adjustment for multiple comparisons
- A full description of the statistical parameters including central tendency (e.g. means) or other basic estimates (e.g. regression coefficient) AND variation (e.g. standard deviation) or associated estimates of uncertainty (e.g. confidence intervals)
- For null hypothesis testing, the test statistic (e.g. F , t , r) with confidence intervals, effect sizes, degrees of freedom and P value noted
Give P values as exact values whenever suitable.
- For Bayesian analysis, information on the choice of priors and Markov chain Monte Carlo settings
- For hierarchical and complex designs, identification of the appropriate level for tests and full reporting of outcomes
- Estimates of effect sizes (e.g. Cohen's d , Pearson's r), indicating how they were calculated

Our web collection on [statistics for biologists](#) contains articles on many of the points above.

Software and code

Policy information about [availability of computer code](#)

Data collection

All code is available for use/re-use at https://github.com/WeitzGroup/covid_shield_immunity in Matlab, Julia, and R. Versions used were MATLAB v2019a, Julia v1.3.1, and R v3.6.0. Permanent link is available at <https://zenodo.org/record/3747685#.XpiEBINKjxs>.

Data analysis

US census bureau data was analyzed in Julia v1.3.1.

For manuscripts utilizing custom algorithms or software that are central to the research but not yet described in published literature, software must be made available to editors/reviewers. We strongly encourage code deposition in a community repository (e.g. GitHub). See the Nature Research [guidelines for submitting code & software](#) for further information.

Data

Policy information about [availability of data](#)

All manuscripts must include a [data availability statement](#). This statement should provide the following information, where applicable:

- Accession codes, unique identifiers, or web links for publicly available datasets
- A list of figures that have associated raw data
- A description of any restrictions on data availability

All simulation codes used in the creation of this manuscript are available at https://github.com/WeitzGroup/covid_shield_immunity. Permanent link is available at <https://zenodo.org/record/3747685#.XpiEBINKjxs>. The US census bureau data is publicly available at https://www2.census.gov/programs-surveys/popest/tables/2010-2018/state/asrh/PEP_2018_PEPSYASEX.zip.

Field-specific reporting

Please select the one below that is the best fit for your research. If you are not sure, read the appropriate sections before making your selection.

- Life sciences Behavioural & social sciences Ecological, evolutionary & environmental sciences

For a reference copy of the document with all sections, see nature.com/documents/nr-reporting-summary-flat.pdf

Life sciences study design

All studies must disclose on these points even when the disclosure is negative.

Sample size	Describe how sample size was determined, detailing any statistical methods used to predetermine sample size OR if no sample-size calculation was performed, describe how sample sizes were chosen and provide a rationale for why these sample sizes are sufficient.
Data exclusions	Describe any data exclusions. If no data were excluded from the analyses, state so OR if data were excluded, describe the exclusions and the rationale behind them, indicating whether exclusion criteria were pre-established.
Replication	Describe the measures taken to verify the reproducibility of the experimental findings. If all attempts at replication were successful, confirm this OR if there are any findings that were not replicated or cannot be reproduced, note this and describe why.
Randomization	Describe how samples/organisms/participants were allocated into experimental groups. If allocation was not random, describe how covariates were controlled OR if this is not relevant to your study, explain why.
Blinding	Describe whether the investigators were blinded to group allocation during data collection and/or analysis. If blinding was not possible, describe why OR explain why blinding was not relevant to your study.

Reporting for specific materials, systems and methods

We require information from authors about some types of materials, experimental systems and methods used in many studies. Here, indicate whether each material, system or method listed is relevant to your study. If you are not sure if a list item applies to your research, read the appropriate section before selecting a response.

Materials & experimental systems		Methods	
n/a	Involved in the study	n/a	Involved in the study
<input checked="" type="checkbox"/>	<input type="checkbox"/> Antibodies	<input checked="" type="checkbox"/>	<input type="checkbox"/> ChIP-seq
<input checked="" type="checkbox"/>	<input type="checkbox"/> Eukaryotic cell lines	<input checked="" type="checkbox"/>	<input type="checkbox"/> Flow cytometry
<input checked="" type="checkbox"/>	<input type="checkbox"/> Palaeontology	<input checked="" type="checkbox"/>	<input type="checkbox"/> MRI-based neuroimaging
<input checked="" type="checkbox"/>	<input type="checkbox"/> Animals and other organisms		
<input checked="" type="checkbox"/>	<input type="checkbox"/> Human research participants		
<input checked="" type="checkbox"/>	<input type="checkbox"/> Clinical data		